ELSEVIER

Finite Elements in Analysis and Design 16 (1994) 317-327

FINITE ELEMENTS IN ANALYSIS AND DESIGN

Boundary conditions for wave propagation problems

J.M. Carcione*

Osservatorio Geofisico Sperimentale, P.O. Box 2011 Opicina, 34016 Trieste, Italy

Abstract

Wave propagation simulation requires a correct implementation of boundary conditions to avoid numerical instabilities. Similar problems are posed by domain decomposition methods where the aim is to find the correct modeling of physical phenomena across the interfaces separating the subdomains. The technique described here is based on physical grounds since it relies on the fact that the wave equation can be decomposed into incoming and outgoing wave modes at the boundary. The result is a modified wave equation for the boundaries which automatically includes the boundary condition. The boundary treatment is applied to a realistic problem of ultrasonic wave propagation through a vertical interface separating an anelastic solid from an elastic solid at the surface. The results show that the method correctly describes the anelastic properties of the Rayleigh wave in the presence of a strong contrast in the material properties.

1. Introduction

The solution of a wave propagation problem is determined by the governing PDEs, the initial conditions, and the boundary conditions. When solving the problem with grid methods, a direct implementation of the boundary conditions may produce instabilities. To avoid this problem a boundary treatment based on characteristics developed by Thompson for fluid dynamic problems [1] is applied to the modeling algorithm. The wave equation, recast as a first-order hyperbolic system, is decomposed into wave modes describing outgoing and incoming waves at the boundaries. The outgoing waves are determined by the solution within the computational volume, while the incoming waves depend on the boundary conditions. In this way, a modified wave equation is solved at the boundaries of the computational domain. The approach allows the simulation of free surface, rigid, non-reflecting, and in general, any arbitrary time-dependent boundary condition.

The boundary treatment is ideal for multipurpose domain decomposition. The interface between two subdomains is considered as a physical boundary where continuity of particle velocities and

*Also at: Geophysical institute, Hamburg University, Bundesstrasse 55, 2000 Hamburg 13, Germany.

SSDI 0168-874X(93)E0101-6

stresses are to be imposed. The method is therefore able to properly simulate solid solid and fluid -solid interfaces separating media with different constitutive equations. A detailed application of the boundary treatment to domain decomposition can be found in [2].

The paper is organized as follows. Section 2 introduces the wave equation in the velocity-stress formulation. The constitutive equation includes isotropic media with dissipation. Section 3 outlines the boundary treatment, and Section 4 recasts the wave equation as an explicit function of the decoupled modes. In Section 5, the method is used to obtain the boundary equations for free surface and non-reflecting conditions, which are implemented in Section 6 to solve a realistic example simulating the reflection and transmission of a Rayleigh wave through a vertical interface in the presence of free surface.

2. The wave equation

The wave equation is based on the equation of momentum conservation combined with the constitutive relations for 2-D isotropic and viscoelastic media [3]; here for simplicity, one dissipation mechanism is considered for each wave mode. The boundary treatment requires a velocity-stress formulation which takes the following matrix form:

$$-\frac{\partial \boldsymbol{v}}{\partial t}+\boldsymbol{A}\frac{\partial \boldsymbol{v}}{\partial x}+\boldsymbol{B}\frac{\partial \boldsymbol{v}}{\partial z}+\boldsymbol{d}=0, \tag{2.1}$$

where

$$\boldsymbol{v}^{\mathrm{T}}=[v_x, v_z, \sigma_{xx}, \sigma_{zz}, \sigma_{xz}, \dot{e}_1, \dot{e}_2, \dot{e}_3], \tag{2.2a}$$

is the vector of unknown variables.

$$\boldsymbol{d}^{\mathrm{T}}=\left[f_x, f_z, (\hat{\lambda}+\hat{\mu})\dot{e}_1+\hat{\mu}\dot{e}_2, (\hat{\lambda}+\hat{\mu})\dot{e}_1-\hat{\mu}\dot{e}_2, \hat{\mu}\dot{e}_3, \frac{-\dot{e}_1}{\tau_\sigma^{(1)}}, \frac{-\dot{e}_2}{\tau_\sigma^{(2)}}, \frac{-\dot{e}_3}{\tau_\sigma^{(2)}}\right]. \tag{2.2b}$$

and

$$\boldsymbol{A}=\begin{bmatrix} 0 & 0 & \rho^{-1} & 0 & 0 & 0 & 0 \\ 0 & 0 & 0 & 0 & \rho^{-1} & 0 & 0 \\ \hat{\lambda}+2\hat{\mu} & 0 & 0 & 0 & 0 & 0 & 0 \\ \hat{\lambda} & 0 & 0 & 0 & 0 & 0 & 0 \\ 0 & \hat{\mu} & 0 & 0 & 0 & 0 & 0 \\ \phi_1 & 0 & 0 & 0 & 0 & 0 & 0 \\ \phi_2 & 0 & 0 & 0 & 0 & 0 & 0 \\ 0 & \phi_2 & 0 & 0 & 0 & 0 & 0 \end{bmatrix}, \quad \boldsymbol{B}=\begin{bmatrix} 0 & 0 & 0 & 0 & \rho^{-1} & 0 & 0 \\ 0 & 0 & 0 & \rho^{-1} & 0 & 0 & 0 \\ 0 & \hat{\lambda} & 0 & 0 & 0 & 0 & 0 \\ 0 & \hat{\lambda}+2\hat{\mu} & 0 & 0 & 0 & 0 & 0 \\ \hat{\mu} & 0 & 0 & 0 & 0 & 0 & 0 \\ 0 & \phi_1 & 0 & 0 & 0 & 0 & 0 \\ 0 & -\phi_2 & 0 & 0 & 0 & 0 & 0 \\ \phi_2 & 0 & 0 & 0 & 0 & 0 & 0 \end{bmatrix}. \tag{2.3 a,b}$$

In the preceding equations, $\boldsymbol{x} = (x, z)$ are the Cartesian coordinates, $v_x(\boldsymbol{x}, t)$ and $v_z(\boldsymbol{x}, t)$ are the particle velocities, $\sigma_{xx}(\boldsymbol{x}, t)$, $\sigma_{zz}(\boldsymbol{x}, t)$, and $\sigma_{xz}(\boldsymbol{x}, t)$ are the stress components, the quantity $e_1(\boldsymbol{x}, t)$ is a field variable related to the dilatational wave, and $e_2(\boldsymbol{x}, t)$ and $e_3(\boldsymbol{x}, t)$ are field variables associated with the shear waves, $\rho(\boldsymbol{x})$ denotes the density, and $\boldsymbol{f}(\boldsymbol{x}, t) = (f_x, f_z)$ are the body forces per unit volume; $\hat{\lambda} = (\lambda + \mu)M_{u1} - \mu M_{u2}$, and $\hat{\mu} = \mu M_{u2}$ are the high-frequency limit or unrelaxed Lame constants, with λ and μ the low-frequency limit or relaxed Lame constants, and $M_{uv} = \tau_\varepsilon^{(v)}/\tau_\sigma^{(v)}$, where $\tau_\varepsilon^{(v)}/\tau_\sigma^{(v)}$ are the material relaxation times: $v = 1$ corresponds to the dilatational mode, and $v = 2$ to the shear modes; finally, $\phi_v = (1 - \tau_\varepsilon^{(v)}/\tau_\sigma^{(v)})/\tau_\sigma^{(v)}$. The anelastic constitutive equation implicit in this formulation is the standard linear solid rheology.

Implementation of the boundary conditions along a given direction requires the characteristic equation corresponding to (2.1) in that direction. This is described in the next Section.

3. The boundary treatment

The method used here was recently developed by Thompson [1], and determines an equation for $\partial \boldsymbol{v}/\partial t$ at the boundaries where the outgoing and incoming waves are decoupled. Let the boundary be normal to the z-direction. Eq. (2.1) can be expressed as

$$-\frac{\partial \boldsymbol{v}}{\partial t} + \boldsymbol{B}\frac{\partial \boldsymbol{v}}{\partial z} + \boldsymbol{c}_z = 0, \quad \text{where } \boldsymbol{c}_z = \boldsymbol{A}\frac{\partial \boldsymbol{v}}{\partial x} + \boldsymbol{d}. \tag{3.1}$$

After diagonalization of matrix $\boldsymbol{B}$ as $\boldsymbol{B} = \boldsymbol{S}\boldsymbol{\Lambda}\boldsymbol{S}^{-1}$, Eq. (3.1) can be written as

$$-\frac{\partial \boldsymbol{v}}{\partial t} + \boldsymbol{S}\mathscr{H} + \boldsymbol{c}_z = 0, \tag{3.2}$$

where

$$\mathscr{H} \equiv \boldsymbol{\Lambda}\boldsymbol{S}^{-1}\frac{\partial \boldsymbol{v}}{\partial z}. \tag{3.3}$$

$\boldsymbol{\Lambda}$ is a diagonal matrix formed with the eigenvalues of $\boldsymbol{B}$, $\lambda_i = 1, \ldots, 8$, therefore $\mathscr{H}$ involves each decoupled characteristic wave mode in the z-direction. Eq. (3.2) completely defines $\partial \boldsymbol{v}/\partial t$ at the boundaries in terms of the decoupled outgoing and incoming modes. The boundary conditions are implemented in the following way. Assume that $a \leqslant z \leqslant b$. For points (x, a), compute $\mathscr{H}_i$ ($\lambda_i < 0$ outgoing waves) from Eq. (3.3), and $\mathscr{H}_i$ ($\lambda_i > 0$ incoming waves) from the boundary conditions. Similarly, for points (x, b), compute $\mathscr{H}_i$ ($\lambda_i > 0$) from Eq. (3.3), and $\mathscr{H}_i$ ($\lambda_i < 0$) from the boundary conditions. Then, solve Eq. (2.1) for the interior region, and Eq. (3.2) at the boundaries.

Gottlieb *et al.* [4], developed a similar way of implementing boundary conditions. They define the characteristic variables vector, say along the z-direction, as

$$\boldsymbol{w} = \boldsymbol{S}^{-1}\boldsymbol{v}, \tag{3.4}$$

such that Eq. (3.2) becomes

$$-\frac{\partial \boldsymbol{w}}{\partial t} + \mathscr{H} + \boldsymbol{S}^{-1}\boldsymbol{c}_z = 0, \quad \text{where } \mathscr{H} = \boldsymbol{\Lambda}\frac{\partial \boldsymbol{w}}{\partial z}. \tag{3.5}$$

It is clear from this equation that $\boldsymbol{w}$ represents decoupled characteristic variables since $\boldsymbol{\Lambda}$ is a diagonal matrix. This approach requires that those components of $\boldsymbol{w}$ corresponding to outgoing characteristic variables remain unmodified after application of the boundary conditions, since these variables have their behaviour entirely defined by the solution inside the physical region. Instead, those components of $\boldsymbol{w}$ corresponding to incoming characteristic variables are determined by the boundary conditions. In this way, the components of $\boldsymbol{v}$, calculated by some scheme using interior points, are corrected in order to fulfil the constraints imposed by the boundary conditions. It can be shown that the method in [4], although using a different formal approach, gives identical results to Thompson's technique. However, the latter has the advantage that the eigenvectors of $\boldsymbol{B}$ corresponding to zero eigenvalues need not be calculated.

4. The boundary equations

Each non-zero quantity in Eq. (3.3) takes the following form:

$$\mathscr{H}_{1(2)} = \frac{c_P}{\sqrt{2}}\left(\pm \frac{\partial v_z}{\partial z} + \frac{1}{Z_P}\frac{\partial \sigma_{zz}}{\partial z}\right), \tag{4.1a}$$

$$\mathscr{H}_{3(4)} = \frac{c_S}{\sqrt{2}}\left(\pm \frac{\partial v_x}{\partial z} + \frac{1}{Z_S}\frac{\partial \sigma_{xz}}{\partial z}\right), \tag{4.1b}$$

where $c_P = \sqrt{(\hat{\lambda} + 2\hat{\mu})/\rho}$ and $c_S = \sqrt{\hat{\mu}/\rho}$ are the unrelaxed compressional and shear wave velocities, and $Z_P = \rho c_P$, $Z_S = \rho c_S$ are the unrelaxed impedances of the medium. The numbers in parentheses correspond to the minus sign.

On the other hand. Eq. (3.2) can be expressed in components as

$$\dot{v}_x = \frac{1}{\rho}\frac{\partial \sigma_{xx}}{\partial x} + \frac{1}{\sqrt{2}}(\mathscr{H}_3 + \mathscr{H}_4) + f_x, \tag{4.2a}$$

$$\dot{v}_z = \frac{1}{\rho}\frac{\partial \sigma_{xz}}{\partial x} + \frac{1}{\sqrt{2}}(\mathscr{H}_1 + \mathscr{H}_2) + f_z, \tag{4.2b}$$

$$\dot{\sigma}_{xx} = (\hat{\lambda} + 2\hat{\mu})\frac{\partial v_x}{\partial x} + \frac{1}{\sqrt{2}}\frac{\hat{\lambda}}{c_P}(\mathscr{H}_1 - \mathscr{H}_2) + (\lambda + \mu)\dot{e}_1 + \mu\dot{e}_2, \tag{4.2c}$$

$$\dot{\sigma}_{zz} = \hat{\lambda}\frac{\partial v_x}{\partial x} + \frac{Z_P}{\sqrt{2}}(\mathscr{H}_1 - \mathscr{H}_2) + (\lambda + \mu)\dot{e}_1 - \mu\dot{e}_2, \tag{4.2d}$$

$$\dot{\sigma}_{xz} = \hat{\mu}\frac{\partial v_z}{\partial x} + \frac{Z_S}{\sqrt{2}}(\mathscr{H}_3 - \mathscr{H}_4) + \mu\dot{e}_3, \tag{4.2e}$$

$$\ddot{e}_1 = \phi_1\left[\frac{\partial v_x}{\partial x} + \frac{1}{\sqrt{2}c_P}(\mathscr{H}_1 - \mathscr{H}_2)\right] - \frac{\dot{e}_1}{\tau_\sigma^{(1)}}, \tag{4.2f}$$

$$\ddot{e}_2 = \phi_2\left[\frac{\partial v_x}{\partial x} + \frac{1}{\sqrt{2}c_P}(\mathscr{H}_2 - \mathscr{H}_1)\right] - \frac{\dot{e}_2}{\tau_\sigma^{(2)}}, \tag{4.2g}$$

$$\ddot{e}_3 = \phi_2\left[\frac{\partial v_z}{\partial x} + \frac{1}{\sqrt{2}c_S}(\mathscr{H}_3 - \mathscr{H}_4)\right] - \frac{\dot{e}_3}{\tau_\sigma^{(2)}}. \tag{4.2h}$$

These equations are used at the boundaries normal to the z-direction, where the quantities $\mathscr{H}_i$ representing incoming variables are calculated from the boundary conditions.

5. Boundary conditions

5.1. Free surface boundary condition

At a free surface the force-free boundary conditions imply that the normal stresses are zero at all times. Thus, the initial conditions at the surface should include $\sigma_{zz} = \sigma_{xz} = 0$, say at $z = h = 0$. The incoming waves correspond to $\lambda_2 = -c_P$ and $\lambda_4 = -c_S$. Then, $\mathscr{H}_2$ and $\mathscr{H}_4$ must be computed from the boundary conditions. From Eqs., (4.2d) and (4.2e), σ_{zz} and σ_{xz} will remain zero at the surface if:

$$\mathscr{H}_2 = \mathscr{H}_1 + \frac{\sqrt{2}}{Z_P}\left[\hat{\lambda}\frac{\partial v_x}{\partial x} + (\hat{\lambda} + \mu)\dot{e}_1 - \mu\dot{e}_2\right], \tag{5.1a}$$

$$\mathscr{H}_4 = \mathscr{H}_3 + \frac{\sqrt{2}}{Z_S}\left[\hat{\mu}\frac{\partial v_z}{\partial x} + \mu\dot{e}_3\right]. \tag{5.1b}$$

Substituting $\mathscr{H}_1$ and $\mathscr{H}_3$ from Eqs. (4.1) in (5.1a) and (5.1b), and the results into Eqs. (4.2a–h), yields the boundary equations for the free surface:

$$\dot{v}_x^{(\text{new})} = \dot{v}_x^{(\text{old})} + \frac{1}{Z_S}\dot{\sigma}_{xz}^{(\text{old})}, \tag{5.2a}$$

$$\dot{v}_z^{(\text{new})} = \dot{v}_z^{(\text{old})} + \frac{1}{Z_P}\dot{\sigma}_{zz}^{(\text{old})}, \tag{5.2b}$$

$$\dot{\sigma}_{xx}^{(\text{new})} = \dot{\sigma}_{xx}^{(\text{old})} - \frac{\hat{\lambda}}{(\hat{\lambda} + 2\hat{\mu})}\dot{\sigma}_{zz}^{(\text{old})}, \tag{5.2c}$$

$$\dot{\sigma}_{zz}^{(\text{new})} = 0, \tag{5.2d}$$

$$\dot{\sigma}_{xz}^{(\text{new})} = 0, \tag{5.2e}$$

$$\ddot{e}_1^{(\text{new})} = \ddot{e}_1^{(\text{old})} - \frac{\phi_1}{\hat{\lambda} + 2\hat{\mu}}\dot{\sigma}_{zz}^{(\text{old})}, \tag{5.2f}$$

$$\ddot{e}_2^{(\mathrm{new})} = \ddot{e}_2^{(\mathrm{old})} + \frac{\phi_2}{\hat{\lambda} + 2\hat{\mu}}\,\dot{\sigma}_{zz}^{(\mathrm{old})}, \tag{5.2g}$$

$$\ddot{e}_3^{(\mathrm{new})} = \ddot{e}_3^{(\mathrm{old})} - \frac{\phi_2}{\hat{\mu}}\,\dot{\sigma}_{xz}^{(\mathrm{old})}, \tag{5.2h}$$

where the superscript (old) indicates the variables given by Eq. (2.1), and the superscript (new) refers to the variables of the left-hand side of Eqs. (4.2a–h).

5.2. *Non-reflecting boundary conditions*

Suppose that $z = a = -z_0$ is a boundary of the numerical mesh. Since this is not a physical boundary, the incoming wave must be suppressed to avoid reflections. The incoming variables are $\mathscr{H}_1$ and $\mathscr{H}_3$. The first and third components of (3.5) give the following characteristics equations for $w_1 = (v_z + \sigma_{zz}/Z_P)/\sqrt{2}$ and $w_3 = (v_x + \sigma_{xz}/Z_S)/\sqrt{2}$:

$$-\frac{\partial w_1}{\partial t} + \mathscr{H}_1 + \frac{1}{\sqrt{2}}\left\{\frac{1}{\rho}\frac{\partial \sigma_{xz}}{\partial x} + \frac{1}{\rho c_P}\left[\hat{\lambda}\frac{\partial v_x}{\partial x} + (\hat{\lambda} + \mu)\dot{e}_1 - \mu\dot{e}_2\right] + f_z\right\} = 0, \tag{5.3a}$$

$$-\frac{\partial w_3}{\partial t} + \mathscr{H}_3 + \frac{1}{\sqrt{2}}\left[\frac{1}{\rho}\frac{\partial \sigma_{xx}}{\partial x} + \frac{1}{\rho c_S}\left(\hat{\mu}\frac{\partial v_z}{\partial x} + \mu\dot{e}_3\right) + f_x\right] = 0. \tag{5.3b}$$

These equations contain the time derivatives of the amplitudes of the incoming characteristic waves w_1 and w_3. Imposing constant amplitudes in time to this modes is equivalent to suppressing them. This yields the expressions for $\mathscr{H}_1$ and $\mathscr{H}_3$ from the preceding equations, while $\mathscr{H}_2$ and $\mathscr{H}_4$ are computed from (4.1). Then, substituting $\mathscr{H}$ in Eqs. (4.2a–h) gives at the non-reflecting boundary:

$$\dot{v}_x^{(\mathrm{new})} = \frac{1}{2}\left(\dot{v}_x^{(\mathrm{old})} - \frac{1}{Z_S}\,\dot{\sigma}_{xz}^{(\mathrm{old})}\right), \tag{5.4a}$$

$$\dot{v}_z^{(\mathrm{new})} = \frac{1}{2}\left(\dot{v}_z^{(\mathrm{old})} - \frac{1}{Z_P}\,\dot{\sigma}_{zz}^{(\mathrm{old})}\right), \tag{5.4b}$$

$$\dot{\sigma}_{xx}^{(\mathrm{new})} = \dot{\sigma}_{xx}^{(\mathrm{old})} - \frac{\hat{\lambda}}{2(\hat{\lambda} + 2\hat{\mu})}\,(\dot{\sigma}_{zz}^{(\mathrm{old})} + Z_P\dot{v}_z^{(\mathrm{old})}), \tag{5.4c}$$

$$\dot{\sigma}_{zz}^{(\mathrm{new})} = \frac{1}{2}(\dot{\sigma}_{zz}^{(\mathrm{old})} - Z_P\dot{v}_z^{(\mathrm{old})}), \tag{5.4d}$$

$$\dot{\sigma}_{xz}^{(\mathrm{new})} = \frac{1}{2}(\dot{\sigma}_{xz}^{(\mathrm{old})} - Z_S\dot{v}_x^{(\mathrm{old})}), \tag{5.4e}$$

$$\ddot{e}_1^{(\mathrm{new})} = \ddot{e}_1^{(\mathrm{old})} - \frac{\phi_1}{2(\hat{\lambda} + 2\hat{\mu})}\,(\dot{\sigma}_{zz}^{(\mathrm{old})} + Z_P\dot{v}_z^{(\mathrm{old})}), \tag{5.4f}$$

$$\ddot{e}_2^{(\mathrm{new})} = \ddot{e}_2^{(\mathrm{old})} + \frac{\phi_2}{2(\hat{\lambda} + 2\hat{\mu})}(\dot{\sigma}_{zz}^{(\mathrm{old})} + Z_P \dot{v}_z^{(\mathrm{old})}), \tag{5.4g}$$

$$\ddot{e}_3^{(\mathrm{new})} = \ddot{e}_3^{(\mathrm{old})} - \frac{\phi_2}{2\hat{\mu}}(\dot{\sigma}_{xz}^{(\mathrm{old})} + Z_S \dot{v}_x^{(\mathrm{old})}). \tag{5.4h}$$

These are two particular cases of boundary conditions that will be used in the example of the following subsection, although general time-dependent boundary conditions can be easily introduced by the present technique, for instance, rigid boundary conditions, source implementation through stress boundary conditions, etc.

6. Example

This example shows the performance of the method to implement free surface and non-reflecting boundary conditions. The problem simulates the reflection and transmission of an ultrasonic Rayleigh wave through a vertical interface. The model is displayed in Fig. 1 together with the material properties, corresponding to the low-frequency limit wave velocities, and quality factors at the angular frequency of $\omega = 690$ kHz. The quality factor quantifies the amount of energy dissipation, the lower its value the higher the dissipation, thus, one should expect attenuation of the Rayleigh wave only in the left half-space. The bulk and shear quality factors can be expressed in terms of the relaxation times as $Q_\nu = (1 + \omega^2 \tau_\varepsilon^{(\nu)} \tau_\sigma^{(\nu)})/(\tau_\varepsilon^{(\nu)} - \tau_\sigma^{(\nu)})\omega$. The values of the relaxation times in the left-half space are $\tau_\varepsilon^{(1)} = \tau_\varepsilon^{(2)} = 1.5$ μs, $\tau_\sigma^{(1)} = 1.427$ μs, and $\tau_\sigma^{(2)} = 1.360$ μs.

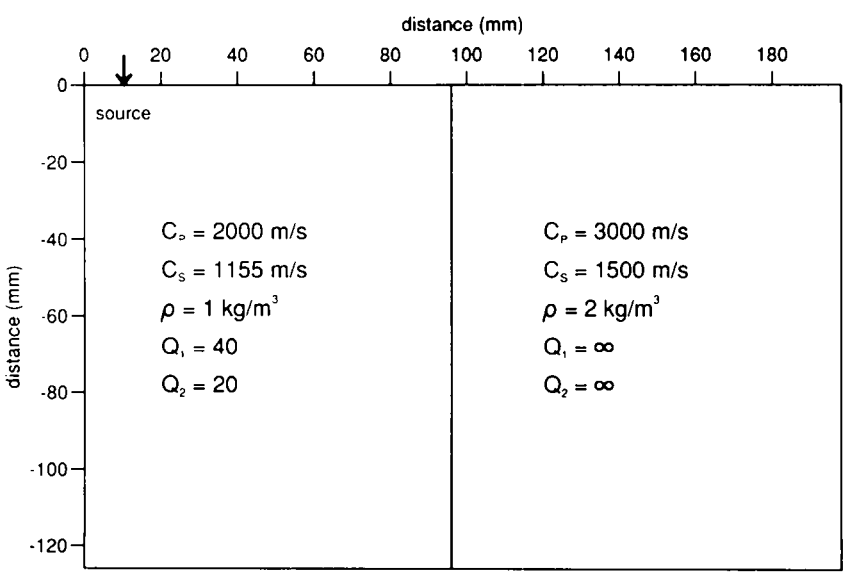

Fig. 1. Model of the vertical interface perpendicular to the free surface. The medium on the left side is anelastic while the medium on the right side is purely elastic. The source is a vertical load with a central frequency of $\omega_0 = 690$ kHz.

The modeling algorithm consists in the calculation of the spatial derivatives, incorporation of the boundary conditions, and time integration. Pseudospectral methods are used to compute the spatial derivatives. In the horizontal direction, the Fourier method is used, then, in this direction the sampling points are equally distributed. However, this method is not appropriate for the vertical direction since it cannot handle the free surface boundary condition properly (this condition implies that the wavefield is not periodic along the vertical direction). Thus, in this direction, the modified Chebychev pseudospectral method is used. The method is non-periodic and provides high accuracy and resolution at the surface. However, when solving the problem with an explicit time marching algorithm, the conventional Chebychev differential operator requires time steps of the order $O(N^{-2})$, where N is the number of grid points. A new algorithm, developed by Kosloff and Tal-Ezer [5] and Tal-Ezer [6], based on a coordinate transformation allows time steps of order $O(N^{-1})$ which are those required also by the Fourier method.

The N_z sampling points are defined by

$$z_i = g(\zeta_i), \quad \zeta_i = \cos(\pi i/N_Z), \qquad i = 0, \ldots, N_Z - 1, \tag{6.1}$$

where ζ_i are the Gauss–Lobato collocation points, and $g(\zeta)$ is a grid stretching function that stretches the super fine Chebychev grid near the free surface in order to have a minimum grid size $D_z = O(N_Z^{-1})$, thus requiring a less severe stability condition. The stretching function used in this problem is

$$g(\zeta) = -|p|^{-1/2}\arcsin\left(\frac{2p\zeta + q}{\sqrt{q^2 - 4p}}\right), \tag{6.2}$$

where $p = 0.5\alpha^{-2}(\beta^{-2} + 1) - 1$ and $q = 0.5\alpha^{-2}(\beta^{-2} - 1)$. Values of $\alpha = 0.06N_Z$, and $\beta = 2$ are used for this example. Fig. 2 represents the conventional and modified Chebychev grids for $N_Z = 20$, respectively. In particular, the density of grid points at the lower boundary has been reduced considerably since a fine grid is not necessary there.

The vertical derivatives are calculated by the chain rule,

$$\frac{\mathrm{d}f}{\mathrm{d}z} = \frac{\mathrm{d}f}{\mathrm{d}\zeta}\frac{\mathrm{d}\zeta}{\mathrm{d}z}, \tag{6.3}$$

The partial derivative $\mathrm{d}\zeta/\mathrm{d}z$ is obtained analytically from (6.2), and the derivative of f with respect to ζ at the ith sampling point is computed via a variant of the fast Fourier transform (FFT) for the cosine transform [7].

The solution is propagated in time by using a fourth-order Runge–Kutta method (e.g. [8]). The time integration scheme computes operations of the type $\boldsymbol{Mv}$ in every step, where

$$\boldsymbol{M} = \boldsymbol{A}\frac{\partial}{\partial x} + \boldsymbol{B}\frac{\partial}{\partial z}. \tag{6.4}$$

within the computational volume as can be seen from Eq. (2.1). Different spatial operators $\boldsymbol{M}_1$ and $\boldsymbol{M}_2$ are used at the upper and lower boundaries which introduce the free surface and non-reflecting conditions according to Eqs. (5.2) and (5.4), respectively. Since for non-vertical incidence, the incoming waves are not eliminated completely, an absorbing strip is used at the lower boundary [9]. This combined approach practically removes non-physical reflections from the boundaries of

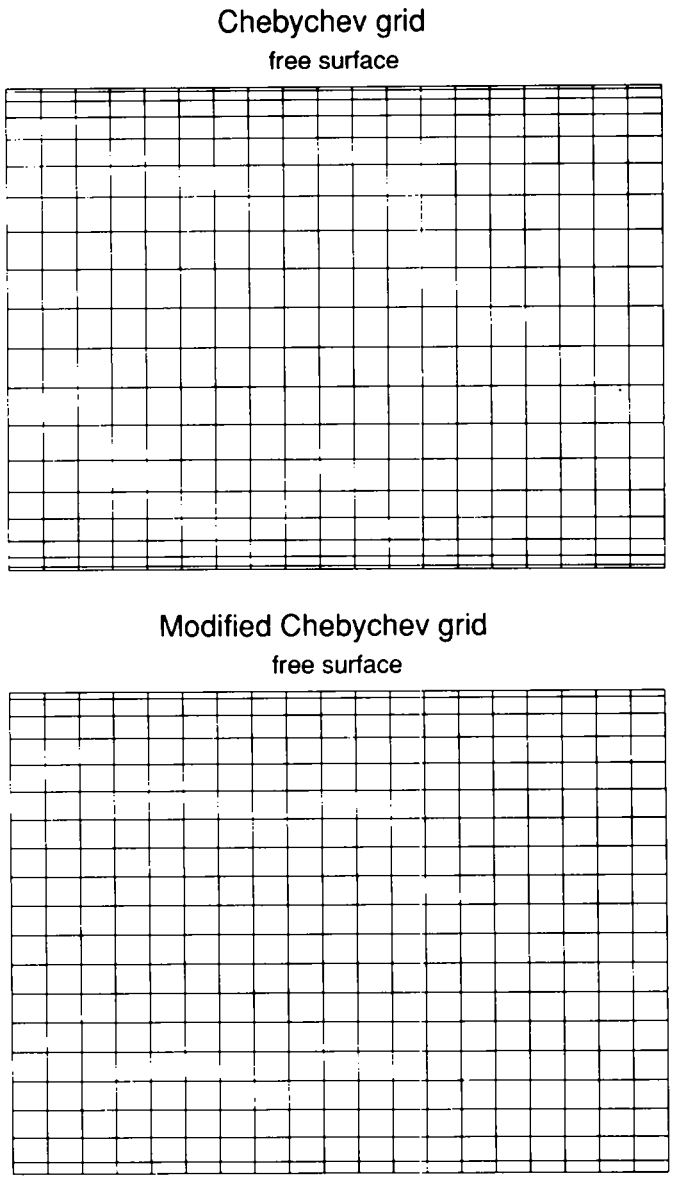

Fig. 2. Chebychev and modified Chebychev grids in the vertical direction. The stretching overcomes the severe stability condition imposed by the conventional Chebychev grid due to the very fine sampling at the boundaries. The Fourier method is used to compute the horizontal derivatives, and therefore the sampling points are equidistant.

the model. Similar absorbing regions are placed along the vertical boundaries to avoid wraparound caused by the periodic properties of the Fourier method.

For the example, the calculations use a grid size of $N_X = 135$ and $N_Z = 81$ with uniform grid spacing $D_X = 2$ mm in the horizontal direction, and a largest vertical grid spacing of $D_z = 2$ mm. A vertical impact whose amplitude spectrum peaks at 690 kHz, where dissipation is maximum, is

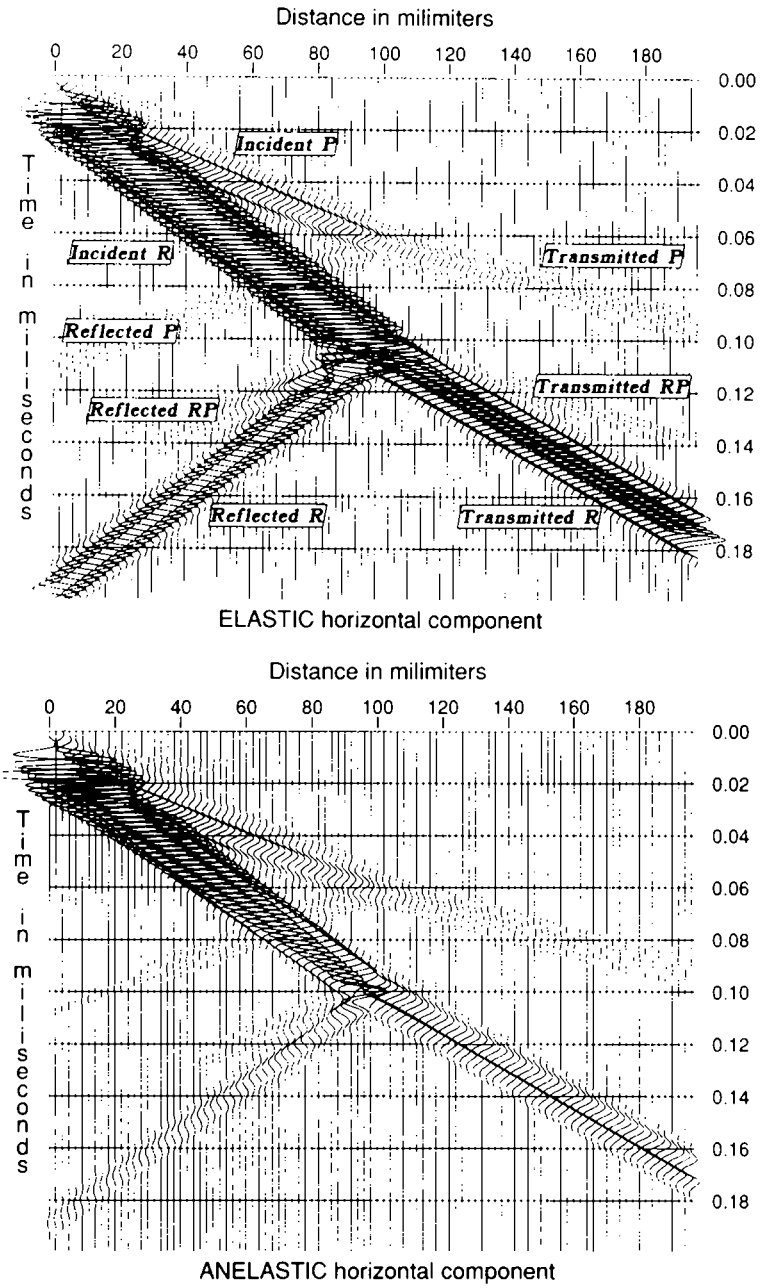

Fig. 3. Comparison between elastic and anelastic v_x time histories recorded at the free surface. It is clear how the boundary treatment properly simulates the behaviour of the ultrasonic Rayleigh wave at both sides of the interface.

applied at the source position. The solution is propagated up to a maximum time of 0.2 ms in time steps of 0.1 μs required by the time-integration scheme.

This example is a good test of the effectiveness of the boundary conditions by observing the properties of the Rayleigh wave at both sides of the vertical interface. Fig. 3 shows v_x recorded along the free surface. The figure compares the elastic and the anelastic time histories where P denotes the compressional wave, R is the Rayleigh wave, and RP is the converted Rayleigh to compressional wave. The latter originates from the collision of the Rayleigh wave with the vertical interface located at approximately 10 cm from the source. It is clear how the incident R surface wave is dissipated in the left side of the interface (up to approximately 0.1 ms travel time), and keeps its amplitude after crossing the interface since the medium is elastic there. On the other hand, the reflected Rayleigh wave attenuates almost completely after 0.2 ms propagating time.

Acknowledgement

This work was supported in part by the Commission of the European Communities under the GEOSCIENCE project.

References

[1] K.W. Thompson, "Time-dependent boundary conditions for hyperbolic systems, II", *J. Comp. Phys.* **89**, pp. 439–461, 1990.

[2] J.M. Carcione, "Domain decomposition for wave propagation problems", *J. Sci. Computing.* **6**, pp. 453–472, 1991.

[3] J.M. Carcione, D. Kosloff and R. Kosloff, "Wave propagation simulation in a linear viscoelastic medium", *Geophys. J. Roy. Astr. Soc.* **95**, pp. 597–611, 1988.

[4] D. Gottlieb, M.D. Gunzberger and E. Turkel, "On numerical boundary treatment for hyperbolic systems", *SIAM J. Numer. Anal.* **19**, pp. 671–682, 1982.

[5] D. Kosloff and H. Tal-Ezer, "A modified Chebychev pseudospectral method with an $O(N^{-1})$ time step restriction", *J. Comp. Phys.* **104**, pp. 457–469, 1993.

[6] H. Tal-Ezer, Non-polynomial spectral method for boundary value problems, *Proc. ICOSAHOM'92 Conf.*, Montpellier, France, 1992.

[7] D. Gottlieb and S.A. Orszag, *Numerical Analysis of Spectral Methods: Theory and Applications*, CBMS Regional Conference Series in Applied Mathematics 26, SIAM, Philadelphia, 1977.

[8] C. Canuto, M.Y. Hussaini, A. Quarteroni and T.A. Zang, *Spectral Methods in Fluid Dynamics*, Springer, Berlin, 1988.

[9] R. Kosloff and D. Kosloff, "Absorbing boundaries for wave propagation problems", *J. Comp. Phys.* **63**, pp. 363–376, 1986.